Photochemical & Photobiological Sciences (2024) 23:339–354
https://doi.org/10.1007/s43630-023-00521-2

ORIGINAL PAPERS

Germicidal efficacy of continuous and pulsed ultraviolet-C radiation on pathogen models and SARS-CoV-2

Anne Sophie Rufyikiri[1] · Rebecca Martinez[1] · Philip W. Addo[1] · Bo-Sen Wu[1] · Mitra Yousefi[2] · Danielle Malo[2,3,4] · Valérie Orsat[1] · Silvia M. Vidal[2,4,5] · Jörg H. Fritz[2,5] · Sarah MacPherson[1] · Mark Lefsrud[1]

Received: 14 July 2023 / Accepted: 12 December 2023 / Published online: 2 February 2024

Abstract

Ultraviolet radiation's germicidal efficacy depends on several parameters, including wavelength, radiant exposure, microbial physiology, biological matrices, and surfaces. In this work, several ultraviolet radiation sources (a low-pressure mercury lamp, a KrCl excimer, and four UV LEDs) emitting continuous or pulsed irradiation were compared. The greatest log reductions in *E. coli* cells and *B. subtilis* endospores were 4.1 ± 0.2 (18 mJ cm^{-2}) and 4.5 ± 0.1 (42 mJ cm^{-2}) with continuous 222 nm, respectively. The highest MS2 log reduction observed was 2.7 ± 0.1 (277 nm at 3809 mJ cm^{-2}). Log reductions of SARS-CoV-2 with continuous 222 nm and 277 nm were $\geq 3.4 \pm 0.7$, with 13.3 mJ cm^{-2} and 60 mJ cm^{-2}, respectively. There was no statistical difference between continuous and pulsed irradiation (0.83–16.7% [222 nm and 277 nm] or 0.83–20% [280 nm] duty rates) on *E. coli* inactivation. Pulsed 260 nm radiation (0.5% duty rate) at 260 nm yielded significantly greater log reduction for both bacteria than continuous 260 nm radiation. There was no statistical difference in SARS-CoV-2 inactivation between continuous and pulsed 222 nm UV-C radiation and pulsed 277 nm radiation demonstrated greater germicidal efficacy than continuous 277 nm radiation. Greater radiant exposure for all radiation sources was required to inactivate MS2 bacteriophage. Findings demonstrate that pulsed irradiation could be more useful than continuous UV radiation in human-occupied spaces, but threshold limit values should be respected. Pathogen-specific sensitivities, experimental setup, and quantification methods for determining germicidal efficacy remain important factors when optimizing ultraviolet radiation for surface decontamination or other applications.

Anne Sophie Rufyikiri and Rebecca Martinez contributed equally to this work.

✉ Mark Lefsrud
mark.lefsrud@mcgill.ca

[1] Department of Bioresource Engineering, Macdonald Campus, McGill University, 21111 Lakeshore Road, Sainte-Anne-de-Bellevue, QC H9X 3V9, Canada

[2] Dahdaleh Institute of Genomic Medicine and McGill University Research Centre on Complex Traits, Life Sciences Complex, McGill University, 3649 Promenade Sir William Osler, Montreal, QC H3G 0B1, Canada

[3] Department of Medicine, McGill University, 3649 Promenade Sir William Osler, Montreal, QC H3G 0B1, Canada

[4] Department of Human Genetics, McGill University, 3649 Promenade Sir William Osler, Montreal, QC H3G 0B1, Canada

[5] Department of Microbiology and Immunology, McGill University, 3775 Rue University, Montreal, QC H3A 2B4, Canada

Graphical abstract

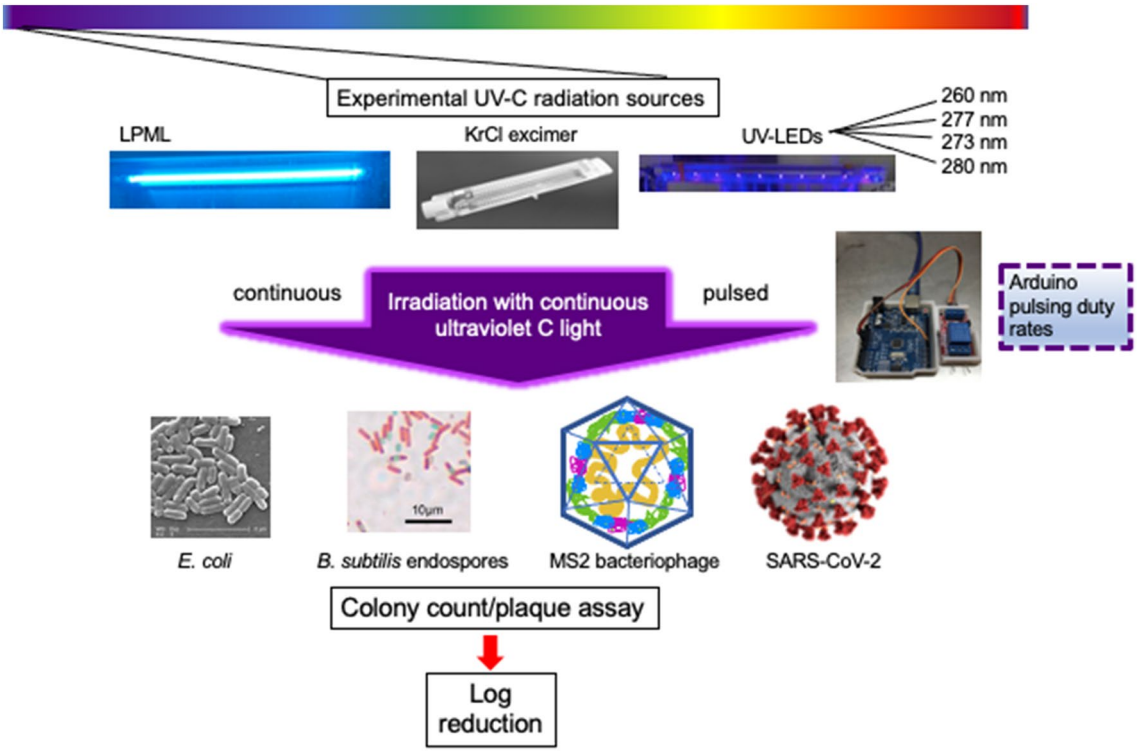

Keywords Disinfection · Light-emitting diode · Pulsed irradiation · Ultraviolet germicidal irradiation · SARS-CoV-2

1 Introduction

Endless biological warfare exists between pathogens and human immunity. Yet, history has shown that decontamination protocols may aid in reducing viral transmission, as demonstrated with severe acute respiratory syndrome coronavirus 2 (SARS-CoV-2) [1]. As the aftermath of the COVID-19 pandemic continues to unfold, data indicate that SARS-CoV-2 can survive on surfaces for days [2–4]. This underlines the urgent need for efficient high touch surface disinfection or equipment sterilization methods in health care settings and public indoor spaces. Of these, the use of ultraviolet (UV) germicidal irradiation (UVGI) has been renewed with pressing interest for this and future pandemics, and new UV-containing devices have exploded into the marketplace. Regulatory bodies in North America, namely, the FDA and Health Canada, have issued technical requirements, display panel obligations, and warnings to manufacturers and consumers to address unproven efficacy claims for disinfection of SARS-CoV-2, while warning of significant risk, direct or indirect, to health, safety, or the environment when using UV radiation-emitting devices [5, 6].

The impact of light on microorganisms was first reported in the late 1800s, as it was determined that sunlight impeded microbial growth within experimental test tubes [7]. Photobiologists have since elucidated that UVGI primarily and directly induces the formation of lethal nucleic acid-damaging pyrimidine dimers, as well as indirectly causing reactive oxygen species (ROS)-mediated damage to lipids, proteins, and cell membranes [8–10], effectively inactivating fungal cells and spores, vegetative bacteria and bacterial endospores, protozoans, and some viruses [11, 12]. Lethal UV-C (200–280 nm) photochemical damage is primarily caused by maximum absorbance by nucleic acids (DNA/RNA) at 260 nm and proteins at 280 nm, while mounting evidence points toward the generation of membrane-damaging ROS and damage inflicted by 222 nm emitting radiation sources on proteins, phospholipids, and glycoproteins found in some viral envelopes [12–14]. Germicidal efficacy is consequently and further dependent on pathogenic species or viruses present, microbial physiology, genome and nucleic acid repair mechanisms, UV radiant exposure (dosage), illumination temperature, and surface types or biological matrices as reviewed elsewhere [15].

Mercury UV lamps represent the most long-standing and conventional delivery of UVGI for medical applications, yet

they are accompanied by many challenges, namely, dangerous leaks, long activation warm-ups, short lifespans, and limited effective radiation areas [16]. Filtered krypton chloride (KrCl) excimers emitting UVGI with a 222 nm peak have attracted much attention recently; this wavelength's germicidal efficacy against Gram-positive and Gram-negative bacteria, bacterial endospores, yeast, and fungi, as well as herpes simplex virus, aerosolized influenza human coronaviruses (HCoV-229E and beta HCoV-OC43) has been reported [12, 14, 17]. SARS-CoV-2-contaminated surfaces are additionally disinfected with 222 nm UV radiation [18]. This may prove favorable for living spaces, as this wavelength does not induce any significant cytotoxic effects in mammalian skin models and mice [19], nor erythema (sunburn) for human skin [20]. Energy-efficient UV LEDs (light-emitting diodes) are advantageous as they allow for the manipulation of different peak wavelengths, potentially targeting different pathogens or enhancing direct and indirect inactivation mechanisms for different applications [16]. The use of UV LEDs has increased in recent years with advantages that include lower power usage, adaptable design configurations, wavelength combination, pulsing, and enhanced robustness [21, 22]. Pulsed UV radiation (100–380 nm) has been implemented in different scenarios for several decades [22, 23], and inactivation of microorganisms (bacteria, yeast, viruses, protozoans, and algae) has been well documented for wastewater treatment, preserving food and in hospitals [24–27]. Pulsed irradiation configurations can be easily achieved with UV LEDs, potentially reducing energy consumption while maintaining germicidal effects, and minimizing exposure to UV radiation**.**

UVGI devices reached unprecedented popularity with the COVID-19 pandemic, yet this technology is fraught with numerous false claims regarding efficacy in inactivating SARS-CoV-2 virus [28]. Safety concerns have been accompanied by reports of photokeratitis and erythema associated with misused UVGI devices or insufficient personal protective equipment against UVGI [29, 30]. Concerns over UV photobiology safety and ozone-producing wavelengths (< 200 nm) from UVGI are not new, and current threshold limit values (TLVs) have been set by the American Conference of Governmental Industrial Hygienists [31]. With increased use, new and separate TLVs for lasers, eyes, and skin are in development or have been proposed [31–33]. These can contribute to the basis of new regulations for occupational hazards, UVGI devices, and lighting installations aimed toward disinfection of high touch surfaces and indoor air in public spaces. Many questions remain around incorporating UV radiation into disease prevention strategies for every day settings, or in pandemic readiness road maps against WHO-prioritized pathogens and 'Disease X' [34]. Given the range of potential applications to mitigate transmission and infection of different airborne, foodborne, waterborne, and occupationally transmitted diseases, concise and scenario-specific regulations for UVGI are required, with prioritized consideration given to TLV, safety, and efficacy.

2 Materials and methods

2.1 UV-C radiation sources

An LPML incorporated into a laminar flow hood (Forma Scientific, Thermo Forma 1845, Waltham, US), a 222 nm KrCl excimer lamp (Excimer-222, Guangdong Excimer Optoelectronic Co., Jiangmen City, China), and four UV LED radiation modules emitting different peak wavelengths across the UV-C range (220–280 nm) were procured for this study from U Technology Corporation (Calgary, AB, Canada) and EHC Global Inc. (Oshawa, ON, Canada). Peak wavelengths for all six lighting installations were measured using an Apogee spectroradiometer (PS-300, Apogee, Logan, UT, US) normalized to 1, and are depicted in Fig. 1. Peak wavelengths confirmed for these manufactured UV-C radiation sources were as follows: 222 nm (KrCl excimer), 254 nm (LPML), 260 nm (UV LED), 273 nm (UV LED, 277 nm (UV LED), and 280 nm (UV LED), respectively.

To measure irradiance (intensity), all radiation sources (with the exception of the LPML in the laminar flow hood, the 277 nm LEDs and the 280 nm UV LEDs) were

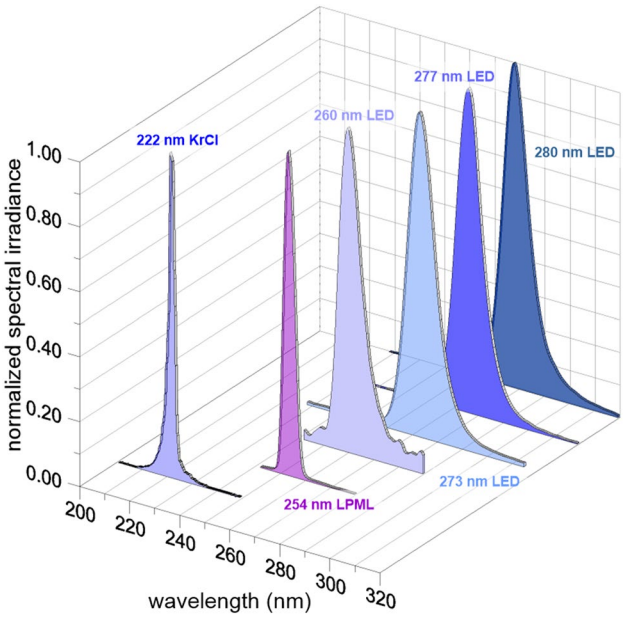

Fig. 1 Spectral distribution and peaks of six UV-C radiation sources normalized to 1 were compared for germicidal efficacy and surface disinfection in this study. *LED* light-emitting diode, *LPML* low-pressure mercury lamp

connected to a power supply (DP832, Rigol Tech, Beaverton, OR, US) then secured with clamps in a laminar flow hood. Heat sinks (Advanced Thermal Solutions Inc., Norwood, MA, US) were incorporated into the experimental setup for the 260 nm and 273 nm UV LEDs to allow for heat dissipation, but this was not possible for the 277 nm and 280 nm UV LED configurations. UV LEDs were turned on and allowed to stabilize (5–10 min). UV-C irradiance and coverage areas were measured and mapped at room temperature (23 °C). Two UV sensors (ILT770-NB and ILT770-UV, International Light Technologies, Peabody, MA, US) were used in these experiments. The ILT770-NB was used for preliminary experiments with the LPML (254 nm). When more UV-C radiation sources were added, this sensor was no longer suitable for measuring irradiance within the greater experimental UV-C range (222–280 nm) and the ILT770-UVwas employed for the other radiation sources. Spectral error of the UV radiation meter for each UV LED configuration was calculated by incorporating the manufacturer's data as described previously to obtain a correction factor for each radiation source [35, 36]). Briefly, to calculate the correction factor with manufacturer's spectral responsive data for all UV-C radiation sources, we used a calculation method previously developed by Ross and Sulev [35] that incorporates the relative spectral sensitivity from a reference pyranometer (in this case ILT770-NB) and the relative spectral sensitivity from the other pyranometer requiring calibration (in this case ILT770-UV), using Eq. 1:

$$\beta_{\mathrm{PYR}} = \frac{\int_{\lambda_{\min}}^{\lambda_{\max}} \varepsilon_{\mathrm{PYR}}(\lambda) \times G^{\mathrm{E}}(\lambda)\mathrm{d}(\lambda) \times \int_{\lambda_{\min}}^{\lambda_{\max}} \varepsilon_{\mathrm{REF}}(\lambda) \times I^{\mathrm{E}}(\lambda)\mathrm{d}(\lambda)}{\int_{\lambda_{\min}}^{\lambda_{\max}} \varepsilon_{\mathrm{REF}}(\lambda) \times G^{\mathrm{E}}(\lambda)\mathrm{d}(\lambda) \times \int_{\lambda_{\min}}^{\lambda_{\max}} \varepsilon_{\mathrm{PYR}}(\lambda) \times I^{\mathrm{E}}(\lambda)\mathrm{d}(\lambda)} \quad (1)$$

where β_{PYR} is the spectral correction, $\varepsilon_{\mathrm{REF}}(\lambda)$ is the relative spectral sensitivity of ILT770-NB, $G^{\mathrm{E}}(\lambda)$ is global radiation, $\varepsilon_{\mathrm{PYR}}(\lambda)$ is the relative spectral sensitivity of ILT770-UV, and $I^{\mathrm{E}}(\lambda)$ is the measured irradiance of each UV-C radiation source. While these measurements were taken, the fluorescent lamp in the laminar hood was turned off, but the fluorescent lighting installation in the laboratory remained on. For each irradiance measurement (three taken for each experimental condition), the sensor was placed so that measured irradiance remained in the same range for all experimental conditions and replicates. For the LPML, irradiance was measured at different predetermined distances from the lamp. LED irradiance was measured prior to each germicidal test to confirm uniformity of radiant exposure testing parameters between experimental replications. The apparent and corrected irradiance levels determined for this study, as well as UV exposure duration and calculated radiant exposure for all UV-C radiation sources, are listed in Table 1.

An Arduino (Arduino, Somerville, MA, US) was used to control the pulsing parameters of the 260 nm and 273 nm UV LEDs. The 222 nm KrCl excimer had a built-in pulsing parameter. EHC Global Inc. provided a built-in controller for the 277 nm and 280 nm UV LEDs, which was used to regulate the pulsing parameters. Pulsed UV-C radiation was emitted with different duty rates (percent of one cycle that the radiation source is on = time radiation source on/time radiation source off × 100) (Table 2), yet with the same total exposure duration (30 s) as continuous radiation (100% duty rate; control) and radiant exposure for each of the UV-C radiation sources was the following: 222 nm KrCl (18.09 mJ cm^{-2}), 260 nm UV LED (2.66 mJ cm^{-2}), 273 nm UV LED (22 mJ cm^{-2}), 277 nm UV LED (63.4 mJ cm^{-2}), and 280 nm UV LED (62.26 mJ cm^{-2}).

2.2 Bacterial strains and viral inocula

Escherichia coli (ATCC 15597; C-3000 derived from K-12), *B. subtilis* (ATCC 23857) and MS2 bacteriophage (ATCC 15597-B1; host *E. coli* C-3000) were obtained from Cedarlane (Burlington, ON). *E. coli* glycerol (20% v/v) stocks were kept frozen at -77 °C and maintained on Luria–Bertani (LB; 1% peptone, 0.5% yeast extract, and 1% NaCl) agar (1.5%) plates. The MS2 bacteriophage was reconstituted in LB as per the manufacturer's instructions (ATCC 15597-B1) and aliquots were kept frozen at -80 °C. The SARS-CoV-2 isolate (Genbank accession no. 599736; lineage B1.1.147) was propagated and titered in Vero E6 cells as described previously [37], following Biological Safety Containment Level 3 (BCL3) procedures.

2.3 Determination of germicidal efficacy

Single colony-forming units (CFU) of *E. coli* were picked from an LB-agar plate to start overnight cultures in LB (25 mL/125 mL Erlenmeyer $flask^{-1}$), shaking with 200 RPM at 37 °C. After 24 h, the optical density of the overnight *E. coli* culture was measured using a spectrophotometer (Ultrospec 2100, Biochrom, Cambridge, UK). Cells (10^8 colony-forming units (CFU) mL^{-1}) were washed and resuspended in phosphate buffered saline (PBS; 137 mM NaCl, 10 mM phosphate, 2.7 mM KCl, pH 7.4). *B. subtilis* endospores were prepared as described previously [38], with some modifications. Difco sporulation media were inoculated (25 mL/125 mL Erlenmeyer flask) with 2–3 CFU and grown for 96 h at 37 °C. Cells were pelleted at 10,000 RPM and resuspended in PBS containing 50 µg lysozyme/mL and incubated 1 h at 37 °C, followed by 10 min at 80 °C. Cells were pelleted for 5 min at 10,000 RPM, washed three times with water, and resuspended in PBS. Endospores were confirmed with malachite green/safranin staining and light microscopy. Working MS2 bacteriophage inocula and dilutions were prepared by freshly diluting stock tenfold in LB. A total of 500 µL *E. coli* cell

Table 1 Radiant exposure determined for continuous UV-C radiation with corresponding duration for all experimental conditions

UV-C radiation source	Irradiance (μW cm^{-2})		Exposure duration (min)		Radiant exposure (mJ cm^{-2})
	Apparent (range; mean ± SD	Corrected (correction factor)			
222 nm KrCl excimer	200–400; 300 ± 50	603 (2.01)	*E. coli*	0.02–2.5	0.6–90.5
			B. subtilis	0.02–2.5	0.7–105.5
			MS2	10.0–60.0	356.4–2138.4
			SARS-CoV-2	0.5–5.0	6.7–180.9
254 nm LPML	1750–2000; 1975 ± 113	1975 (1)	*E. coli*	2.5–10.0	21.6–1050.0
			B. subtilis	0.5–10.0	52.5–1050.0
			MS2	10–60.0	2202.0–13212.0
			SARS-CoV-2	n/a	ND
260 nm UV LED	22–23; 22.5 ± 5.6	88.7 (3.94)	*E. coli*	2.5–10.0	1.5–53.2
			B. subtilis	0.5–30.0	2.7–159.6
			MS2	10.0–60.0	319.1–1843.9
			SARS-CoV-2	n/a	ND
273 nm UV LED	12.2–20.0; 16.1 ± 4.0	559.3 (45.84)	*E. coli*	0.5–10.0	22.1–442.8
			B. subtilis	0.17–10.0	7.38–442.8
			MS2	10.0–60.0	440.1–2656.9
			SARS-CoV-2	n/a	ND
277 nm UV LED	13.5–15; 14.3 ± 3.6	2116.38 (148.52)	*E. coli*	0.5–2.5	60.1–300.7
			B. subtilis	0.2–10.0	44.6–2673.0
			MS2	10.0–60.0	1269.7–7618.5
			SARS-CoV-2	0.5–5.0	60.1–601.4
280 nm UV LED	8.6–9; 8.8 ± 2.2	2075.30 (235.83)	*E. coli*	0.5–2.5	62.3–311.3
			B. subtilis	0.2–10.0	20.8–311.3
			MS2	10.0–60.0	1245.2–7471.1
			SARS-CoV-2	n/a	ND

Apparent irradiance is presented as minimum and maximum values (range), mean, and estimated standard deviation (SD) for all experimental conditions and replicates

n/a not applicable, *LED* light-emitting diode, *LPML* low-pressure mercury lamp, *ND* not determined, *UV* ultraviolet

Table 2 Experimental duty rates (percentage of irradiation duration in each on and off cycle) for pulsed UV-C radiation using the 222 nm KrCl excimer and the 260 nm, 273 nm, 277 nm, and 280 nm UV LEDs, along with corresponding cycles

Duty rate (duration on/duration off × 100)	Irradiation time per minute (s)	Irradiation cycles equaling corresponding period (min)	Total UV exposure duration (s)
(0.2 s/60 s × 100) = 0.33%	0.2	150	30
(0.3 s /60 s × 100) = 0.50%	0.3	100	30
(0.5 s/60 s × 100) = 0.83%	0.5	60	30
(1 s/60 s × 100) = 1.67%	1.0	30	30
(10 s/60 s × 100) = 16.67%	10	3	30
(10 s/50 s × 100) = 20%	10	3	30
(30 s/30 s × 100 = 100%[a]	30	1	30

Pulsed UV-C radiation with the LPML could not be performed as it could not be reconfigured in the laminar flow hood for pulsed irradiation

[a]100% duty rate corresponds to 30 s continuous UV-C radiation (control)

suspension (≅ 10^8 CFU mL^{-1}), 500 μL *B. subtilis* endospore suspension (≅ 10^8 CFU mL^{-1}), or 180 μL freshly diluted MS2 (≅ 10^8 PFU mL^{-1}) or 200–500 μL SARS-CoV-2 (≅ 10^5 PFU mL^{-1}) inocula were placed as a single droplet in an uncovered 100 mm polystyrene Petri dish within a laminar flow hood, where UV-C radiation sources were set up to irradiate microbial suspensions with a predetermined radiant exposure range for each UV-C radiation source. The same radiation method was employed with a diluted stock of the SARS-CoV-2 isolate, performed in a biological safety

cabinet at McGill University's BCL3 facility (Montreal, QC, Canada). Briefly, previously titered SARS-CoV-2 isolate stock was thawed on a cold block, diluted in DMEM as described previously (without fetal bovine serum) prior to irradiation, and 220–500 µL droplets of SARS-CoV-2 inocula ($\cong 10^5$ PFU mL^{-1}) were placed in an open Petri dish. Experimental radiant exposure was determined by setting each UV-C source as close to the testing surface as possible (with exception of the LPML in the laminar flow hood), with at least three different irradiation durations that resulted in ranging radiant exposure for each UV-C radiation source. Controls included the same volumes of *E. coli* cell and *B. subtilis* endospore suspensions, diluted MS2 or SARS-CoV-2 inocula placed in an uncovered Petri dish, and exposed to air for the same exposure duration without any laminar hood illumination.

After irradiation, the Petri dish containing the irradiated *E. coli*, *B. subtilis* endospores, or MS2 inocula was rinsed several times before transferring to a microfuge tube. If volume was lost to air-drying, sterile PBS (or LB for MS2) was added to the suspensions to reach the pre-irradiation volume. For *E. coli* and *B. subtilis*, 100 µL of select serial dilutions was spread in technical replicates on 100 mm Petri dishes containing LB-agar and incubated overnight at 37 °C for approximately 18 h. For MS2, plaque assays were performed using a modified double layer agar technique [39]. CFU and plaque forming units (PFU) were manually counted the next day or with OpenCFU 3.8 image processing software [40] whenever possible. Cold blocks were used to manipulate SARS-CoV-2 during serial dilutions with DMEM (without fetal bovine serum). Plaque enumeration for SARS-CoV-2 was performed in Vero E6 cells and crystal violet staining according to Mendoza et al. [37], in technical replicates. Image capturing and processing was not possible for SARS-CoV-2 PFU in the BCL3 at the time that the experiments were performed. Each experimental condition with *E coli*, *B. subtilis*, MS2, and SARS-CoV-2 was biologically replicated independently three times.

2.4 Data collection and statistical analysis

Germicidal efficacy was analyzed by calculating log reduction (Eq. 2):

$$\text{Logreduction} = \log\left(\frac{N_0}{N}\right), \tag{2}$$

where N_0 and N represent numbers of CFU or PFU counted without UV-C radiation (control) and after UV-C radiation treatments, respectively. The full factorial design was to evaluate the effect of the independent variables on the dependent variables (microbial log reduction). The independent variables consisted of five wavelengths and duty rates. Triplicates of each experimental condition were performed and mean values with standard error means were reported. Analysis of variance (ANOVA) was used to investigate the statistical significance of the regression coefficients by conducting the Fisher's *F*-test at 95% confidence level. The least square multiple regression methodology was used to evaluate the relationship between the independent and dependent variables. Regression analyses were done to evaluate the linear effect of the dependent variables and the quadratic effect of the interaction of the wavelengths and duty rates on the log reduction of the pathogens. Pairwise comparisons of means were done using the Student's *t* test. Different linear and non-linear regression models were evaluated to determine best fit with the collected data. The rational regression model was selected to generate fitted inactivation curves with Prism (Prism Software, Irvine, CA, US), due to low root mean square error (RMSE) and high R^2 values determined with Curve Expert 2.6.5 software using Eq. 3:

$$y = \frac{a + bx}{1 + cx + dx^2}, \tag{3}$$

where y is log reduction, x is radiant exposure (mJ cm^{-2}), and a, b, c, and d are model coefficients (unitless; listed in Supplementary Table 1).

Pulsed irradiation data represent mean values of biologically replicated experiments that were analyzed using JMP software (SAS Institute, Cary, North Carolina, US). A full factorial design was used to test the fitness of the model and the analysis of variance. The Student's *t* test was used for multiple pairwise comparisons for the given UV-C radiation source and duty rates.

3 Results

3.1 Continuous UV-C radiation

The germicidal efficacies of the different radiation sources emitting continuous UV-C radiation were determined against a panel of microorganisms. Log reduction data were used to generate fitted curves (Fig. 2) using the rational non-linear regression model.

Using continuous UV-C radiation, the highest log reduction in *E. coli* CFU obtained was 4.1 ± standard error mean (SEM) of 0.2 with the 222 nm KrCl excimer at a minimum radiant exposure of 18 mJ cm^{-2} (0.5-min exposure). The highest log reduction in *B. subtilis* endospores obtained with minimum radiant exposure was using the 222 nm KrCl excimer (42 mJ cm^{-2}; 1 min) was 4.5 ± 0.1. Greater radiant exposure for all UV-C radiation sources

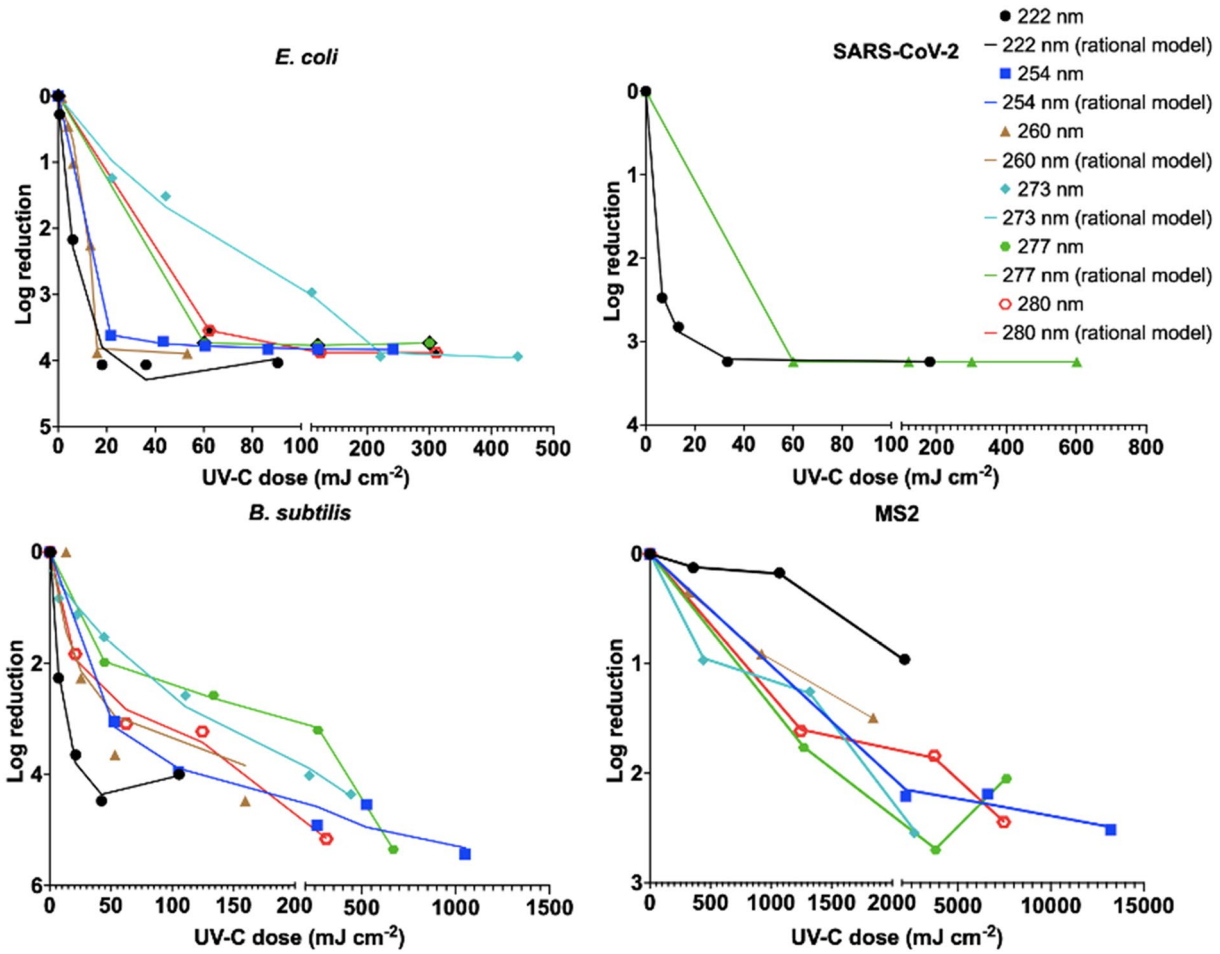

Fig. 2 Fitted curves demonstrating germicidal efficacy (log reduction in CFU or PFU) on suspended *E. coli* (upper left), *B. subtilis* endospores (upper right), MS2 bacteriophage (lower left), and a SARS-CoV-2 isolate (bottom right) with continuous UV-C radiation. Fitted curves were generated with mean values ± standard error mean (SEM) from three biologically replicated experiments

was required to inactivate the MS2 bacteriophage than the bacterial models. The highest log reduction in MS2 PFU obtained with minimum radiant exposure was 2.7 ± 0.1, using the 277 nm UV LED at 3809 mJ cm^{-2} (30-min exposure). For SARS-CoV-2, the highest log reduction in PFU obtained with minimal radiant exposure was 3.4 ± 0.7 with the 222 nm KrCl excimer emitting 13.32 mJ cm^{-2} (30 s exposure). Log reductions > 3.4 were calculated with the 222 nm KrCl UV lamp at higher radiant exposure (33–180 mJ cm^{-2}) and similarly with the 277 nm UV LED with nearly five times the radiant exposure (60 mJ cm^{-2}; 0.5-min exposure) as no PFU were detected in the plaque assays with these UV-C conditions. The rational regression model was used to interpolate and predict radiant exposure (mJ cm^{-2}) required for incremental log inactivation of the experimental microbial panel. Predicted values were extracted for each log reduction (1–4) where applicable (Supplementary Table 2).

3.2 Continuous vs. pulsed UV-C radiation with different duty rates

The germicidal efficacies of continuous and pulsed UV-C radiation with different duty rates (0.33–20%) on *E. coli*, *B. subtilis* endospores, and SARS-CoV-2 inocula were compared using the same total exposure duration (30 s) and radiant exposure for each UV-C radiation source. These were compared to 30 s continuous irradiation (considered a 100% duty rate and serving as the control) for all the UV-C radiation sources, with exception of the LPML. Log reductions in CFU (*E. coli* and *B. subtilis*) or PFU (SARS-CoV-2) are plotted in Figs. 3, 4, and 5.

No statistical difference between continuous and pulsed irradiation (0.83–16.7% at 222 nm and 277 nm or 0.83–20% for 280 nm) on *E. coli* inactivation was observed. The highest log reduction in *E. coli* CFU obtained was 3.9 ± 0.1 with the 277 nm UV LED (63.40 mJ cm^{-2}), at a duty rate of 20%. In comparison, continuous UV-C radiation (100%

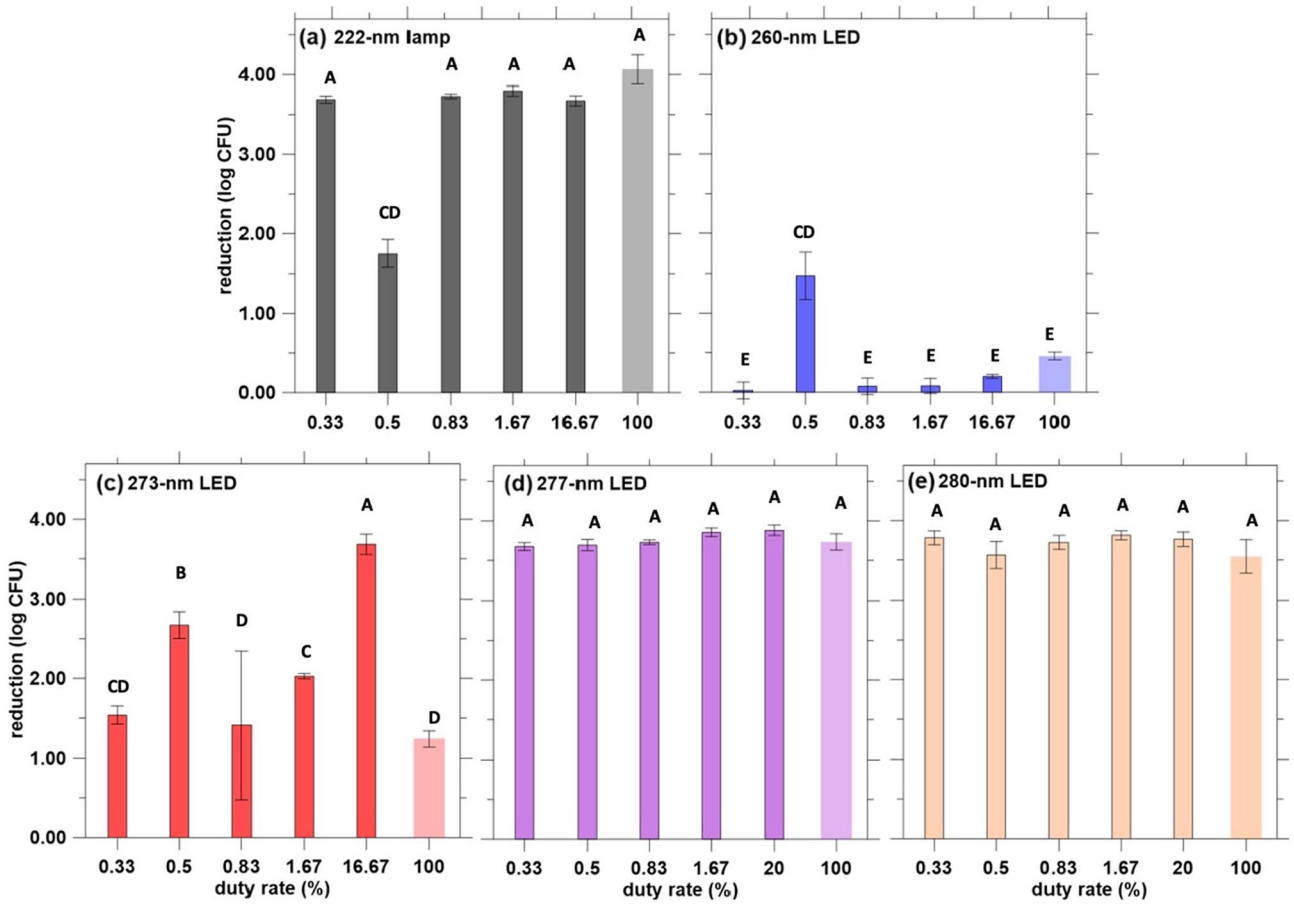

Fig. 3 Log reduction of *E. coli* with pulsed UV-C radiation under the same radiant exposure with different duty rates (0.33–100%) where a 100% duty rate corresponds to 30 s continuous radiation (control). Radiant exposure for each UV-C radiation source was as follows: 222 nm KrCl (18.09 mJ cm^{-2}), 260 nm UV LED (2.66 mJ cm^{-2}), 273 nm UV LED (22 mJ cm^{-2}), 277 nm UV LED (63.4 mJ cm^{-2}), and 280 nm UV LED (62.26 mJ cm^{-2}). Bars represent mean values ± SEM (standard error mean) from three biologically replicated experiments. Values not connected by the same letter for **a**–**e** are significantly different

duty rate) with the same UV LED resulted in an *E. coli* CFU log reduction of 3.7 ± 0.1. For *B. subtilis* endospores, pulsed 277 nm UV LED radiation (63.40 mJ cm^{-2}) resulted in a significantly higher log reduction (4.28 ± 0.10) at a duty rate of 0.83% than continuous UV-C radiation with the same UV LED (2.58 ± 0.23). Pulsed UV-C radiation (0.5% duty) at 260 nm yielded significantly greater log reduction for both *E. coli* and *B. subtilis* than continuous radiation with the same UV LED. At 222 nm, there was no statistical difference in SARS-CoV-2 inactivation between continuous and pulsed irradiation. Pulsed 277 nm UV-C radiation (63.40 mJ cm^{-2}) resulted in a significantly higher log reduction (5.1 ± 0.3 with 1.7% duty rate) than continuous UV-C radiation with the same UV LED (100% duty rate; log reduction of 3.5 ± 0.0). No direct comparison between continuous and pulsed irradiation on MS2 could be made as continuous exposure duration started at 10 min; however, log reduction data collected for tested pulsed irradiation conditions on MS2 are listed in Supplementary Table 3.

4 Discussion

UVGI is a non-thermal and non-chemical control method widely used to assure the quality and safety of food or water, as well as sterilization of medical devices. In the wake of the COVID-19 pandemic, UVGI sources claiming high-level disinfection for reusable medical devices must ensure a minimum 6 log reduction (99.9999% reduction) to comply with Health Canada and FDA requirements [6, 28, 41]. Commercial products intended for decontamination of rooms, environmental surfaces or household products typically attain a lower level of disinfection (3-log reduction or 99.9% reduction)[42]. The aim of the present study was to investigate and compare the germicidal efficacies of six UV-C radiation sources on three surrogate pathogens and a SARS-CoV-2 isolate. These radiation sources included one LPML incorporated into a laminar flow hood, one KrCl excimer, and four UV LED radiation modules undergoing screening for prospective inclusion in a commercial lighting installation

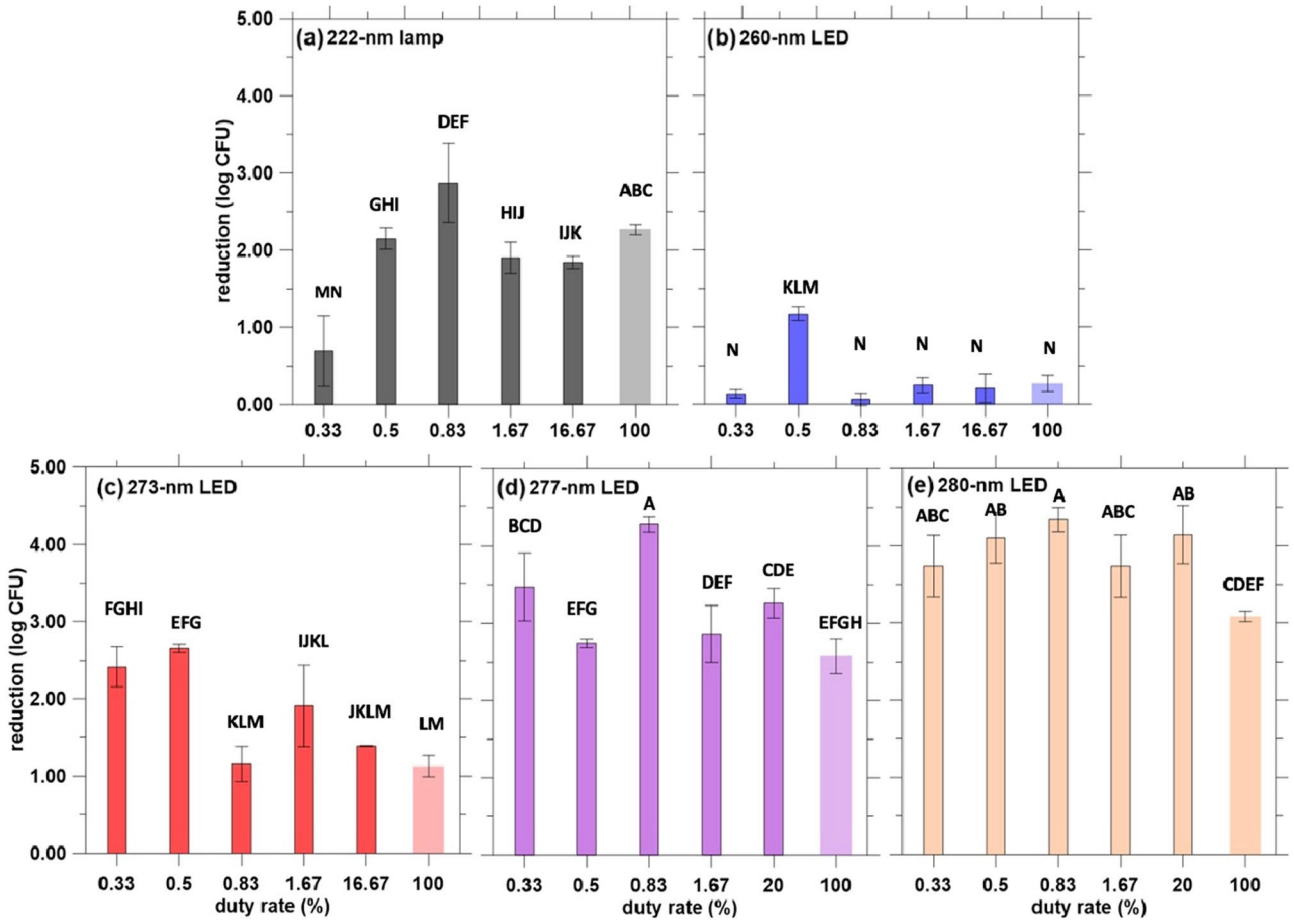

Fig. 4 Log reduction of *B. subtilis* with pulsed UV-C radiation under the same radiant exposure with different duty rates (0.33–100%) where a 100% duty rate corresponds to 30 s continuous radiation (control). Radiant exposure for each UV-C radiation source was as follows: 222 nm KrCl (18.09 mJ cm^{-2}), 260 nm UV LED (2.66 mJ cm^{-2}), 273 nm UV LED (22 mJ cm^{-2}), 277 nm UV LED (63.4 mJ cm^{-2}), and 280 nm UV LED (62.26 mJ cm^{-2}). Bars represent mean values ± SEM (standard error mean) from three biologically replicated experiments. Values not connected by the same letter for **a**–**e** are significantly different

for surface disinfection. Evidence reported to date suggests it may be possible to optimize germicidal efficacy by selecting UV LEDs with specific peak emission wavelengths, as LEDs can often provide additional advantages over conventional UV-C radiation sources, including safety, energy efficiency, longer lifespan, flexibility with respect to different applications and installation, as well as controllability [43]. The inclusion of a 222 nm KrCl excimer was justified by trending research indicating that deep UV-C (207–235 nm) appear safe for mammalian skin, eyes, and living spaces [19, 44–46]. Continuous and pulsed UV-C radiation was further compared to contrast these two irradiation delivery methods.

Comparing the germicidal efficacy of the experimental UV-C radiation sources emitting continuous irradiation emphasized wide-ranging sensitivities and differences in radiant exposure required to achieve high log reductions. Inactivation of suspended *E. coli* cells and *B. subtilis* endospores achieved with the 222 nm KrCl excimer in this work supports germicidal efficacies reported previously, in which DNA damage (not protein damage) was the primary UV-induced inactivation mechanism against *E. coli* and endospore-forming bacilli [12, 17]. Germicidal efficacies for surface decontamination of SARS-CoV-2 range from 88.5 to 99.7% with 1 mJ cm^{-2} and 3 mJ cm^{-2} [47]. A differently sourced KrCl excimer (222 nm) showed limited germicidal activity against SARS-CoV-2 at 280 µJ cm^{-2}, achieving < 2-log reduction using $TCID_{50}$ and immunofluorescence detection assays [48]. Approximately 6.7 mJ cm^{-2} was used to achieve a > 3-log reduction in this study, measured by manually enumerated plaque assays. Limited time and equipment permitted in the BCL3 facility did not allow for germicidal testing against SARS-CoV-2 with the other manufactured UV-C sources. It was noted that predicted radiant exposure for the 222 nm KrCl excimer required the lowest radiant exposure in inactivating both bacterial strains and SARS-CoV-2, yet it was inefficient and unable to attain

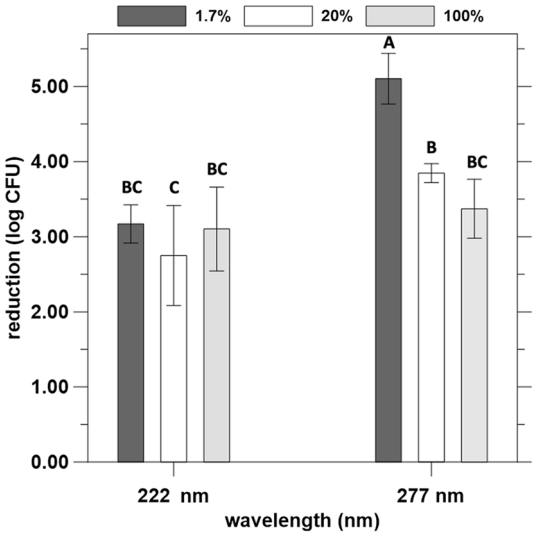

Fig. 5 Log reduction of SARS-CoV-2 with pulsed UV-C radiation under the same radiant exposure with different duty rates: (1.7–20%) where a 100% duty rate corresponds to 30 s continuous radiation (control). Radiant exposure was 18.09 mJ cm^{-2} for the 222 nm KrCl excimer and 63.4 mJ cm^{-2} for the 277 nm UV LED. Bars represent mean values ± SEM (standard error mean) from three biologically replicated experiments. Values not connected by the same letter are significantly different

a 2-log reduction in the non-enveloped virus surrogate MS2 with these experimental conditions. Continuously emitted 260 nm UV LED radiation similarly performed poorly with MS2, as did the 222 nm KrCl excimer, achieving a < 2-fold log reduction with the highest experimental radiant exposure (2138 mJ cm^{-2}). This contradicts MS2 inactivation reported elsewhere with a similar KrCl excimer lamp, where a > 5-fold log reduction with only 50 mJ cm^{-2} was reported [49]. It is possible that different inactivation dosages with similar UV-C radiation sources can be attributed to varied experimental methods, including radiation properties (irradiance, working distance, angle, reflectivity, etc.), as well as different test surfaces, matrices, and assays to quantify log reduction values reviewed elsewhere [50].

Considerably more radiant exposure with other wavelengths was similarly needed to inactivate the MS2 bacteriophage in this work. The 260 nm UV LED performed poorly and this was unexpected, considering optimal wavelengths for inactivating MS2 range from 253–265 nm, with higher sensitivity below 240 nm and at 260 nm [11, 21, 51]. Poor performance could be caused by this particular UV LED's low irradiance. Although UV damage to bacteriophage proteins could contribute to the loss of infectivity observed at lower wavelengths via amino acid absorption, loss of MS2 infectivity appears primarily caused by damage inflicted to its viral RNA genome [11, 52]. A comparison between continuous and pulsed UV-C radiation was not possible, as exposure required for a quantifiable log reduction required at least 10 min (and greater radiant exposure) for most UV-C radiation sources. The appropriateness of MS2 bacteriophage as a surrogate non-enveloped virus has been questioned, given dissimilarities in viral coat proteins and different mechanisms of UV inactivation [11]. Its use as a model virus for aerosol studies has further been scrutinized as MS2 shows more resistance to aerosolization and sampling than other bacteriophages, highlighting the importance of selecting suitable models for aerosol-transmitted human and animal viruses [53]. Several bacteriophages were recently used as non-enveloped (MS2 and PPhiX174) and enveloped (Phi6) virus models for the rapid coronavirus decontamination of a high touch surface with UV-C radiation; > 2-fold log reductions were reported for MS2, compared with > 3-fold log 10 reductions of PhiX174 and Phi6 using a LPML at 25,560 mJ cm^{-2} [54]. Further experimentation is recommended for MS2 if it is to be used as a surrogate using KrCl excimer lamps.

Several studies have demonstrated that UV-C radiation sources, including a LPML, KrCl excimer, and UV LEDs, are relatively effective at irradiating SARS-CoV-2 and inhibiting viral replication [14, 47, 55–57]. Reported log reductions for SARS-CoV-2 with a KrCl excimer lamp range from < 1 log (88.5% reduction) to 4 log (99.99% reduction) with 1 mJ cm^{-2} and 8 mJ cm^{-2}, respectively [47, 58]. One study shows that an unfiltered KrCl excimer with a primary peak at 222 nm and another 270 nm peak had the highest disinfection rate when irradiating SARS-CoV-2 compared to a LPML emitting at 254 nm and LEDs emitting at 270 nm and 282 nm [14]. A portable 275 nm UV LED device can reportedly achieve a 4-log reduction (99.99% reduction when irradiated with more than 10 mJ cm^{-2}). In comparison, a radiant exposure of 13 mJ cm^{-2} with the 222 nm KrCl lamp and 60 mJ cm^{-2} with the 277 nm UV LED were required to achieve log reductions ≥ 3.37 ± 0.68 for SARS-CoV-2 in this study. Factors related to cell culture could further affect viral inactivation, as differential inactivation of human coronaviruses, including SARS-CoV-2, suspended in cell media containing fetal bovine serum or buffers have been reported [57, 59, 60]. The effectiveness of UV-C on inactivating wet versus dried droplets containing SARS-CoV-2 on surfaces is another important consideration [61]. This factor was not parsed in this work, yet it was controlled with microbe-containing droplets exposed to air for the same duration without radiation. Inocula, suspension, and survival time in experimental buffers, in biological materials and on surfaces, whether for bacteria or viruses should equally be considered, as previous research has demonstrated that these factors can impact viability over long periods of time [3, 59, 62–65]. Difficulties in delivering uniform UV dosage and optical phenomena such as radiation profiles and reflection at surface may further hinder

microbial inactivation [66]. In a recent critical analysis, the occurrence of non-linear models in microbial inactivation was attributed to studies where no further inactivation was observed at high irradiance, exhibited by a tailing effect [67]. This has been previously debated for inclusion in microbial inactivation models [68]. Non-linearity has additionally been reported when microbial inactivation could not be achieved at very low irradiance, and before log reduction can be detected, which may be exhibited by shouldering. Plotted microbial inactivation and models can further be affected by microbial or microbial-particle aggregation, shielding, absorbing, and scattering or blocked UV radiation, in addition to four correction factors when monochromatic radiation is considered: the Petri factor, reflection, water, and divergence [69]. However, it may be inappropriate to use the Petri factor for UV LED experiments [67] and other correction factors in the current experimental design for surface decontamination where small volume droplets were used. It is important to note that biological factors that might alter microbial activation, such innate and acquired UV resistance, were not considered in our analyses. The use of quantitative CFU enumeration methods plaque assays over $TCID_{50}$ determination of viral inactivation may further affect microbial activation and this model, and starting bacterial or viral stock, subsequent post-radiation dilutions, and absence of CFU or PFU likely indicate our limit of detection with these assays, and not necessarily the highest log reduction that can be achieved. Innovative molecular detection, quantification, and titration methods, some of which are antibody based, may prove faster, more cost effective and reliable for experimental settings [64, 70–72]. Imaging software produced similar *E. coli* and *B. subtilis* CFU data in this study, yet it was not useful for MS2 and the BLC3 facility was not equipped with cameras to capture SARS-CoV-2 plaque images at this time. Nonetheless, UV inactivation or sterilization remains an established tool in the laboratory, and UV LEDs' flexible and controllable designs may serve as alternate instruments with longer lifespan.

Greater radiant exposure was required for *E. coli* inactivation with the 273 nm, 277 nm and 280 nm UV LEDs compared to the KrCl excimer and the LPML in this study. For *B. subtilis* endospores, the KrCl excimer lamp achieved comparable log reduction with less radiant exposure. Bacterial membrane integrity could be more compromised at 279 nm than at 266 nm, as proteins display peak absorbance at approximately 280 nm; although DNA damage inflicted at lower UV-C wavelengths remains the primary inactivation mechanism, higher peak wavelength irradiation may induce greater membrane protein vulnerability and contribute to germicidal efficacy [9]. Studies using dual UV-C wavelengths (260 nm/280 nm) did not report any synergies for inactivation of *E. coli*, *Bacillus pumilus* endospores, MS2, human adenovirus type 2, and several enteroviruses [21, 73], while sequential UV-C radiation with LPML and a KrCl excimer lamp improved germicidal efficacy for MS2 [49].

Data presented here suggest that pulsed UVGI may prove superior to continuous UVGI in some scenarios, yet for all wavelengths, varying duty rates often dictated germicidal efficacy with no apparent trend. Past studies using pulsed irradiation were initially conducted with xenon lamps with different microorganisms within the context of food safety, water treatment, and disinfection in hospitals [27, 74, 75]. Barbosa-Canovas et al. reported xenon pulses emitting 1–20 flashes per second, illustrating differences in spectral distribution, frequency, irradiance, and duty rate in comparison to LEDs [23]. More recently, the germicidal efficacy of a UV low-pressure lamp, as well as 265 nm and 285 nm UV LEDs, was investigated with different pulsed duty rates on *E. coli* and MS2; the 265 nm UV LED performed significantly better for all duty rates than the UV low-pressure lamp [76]. Our findings are consistent with this report, as varying duty rates for the 280 nm UV LEDs still achieved the same log reduction for *E. coli* and *B. subtilis*. At least two other studies suggest that pulsed irradiation inactivates pathogens more effectively than continuous irradiation [74, 77], while others showed no significant difference [22, 78, 79]. Given MS2's apparent resistance to UV inactivation in this investigation, future work could explore the germicidal effects of pulsed UV-C on MS2 over a prolonged period (i.e., 24 h), instead of the 30 s used here.

Certain microbes' nucleic acid repair abilities might counteract the germicidal efficacy of UV radiation, as some evidence suggests that pulsed irradiation may be advantageous, as higher irradiance in short bursts might render repair enzymes sensitive [80, 81]. Specific radiation wavelengths may further prove optimal, as 270 nm UV LEDs have higher efficacy for inhibiting nucleic acid repair [82]. Irrespective of a pathogen's ability to repair nucleic acid damage, pulsed irradiation avoids heat damage caused by temperature increase [22], preventing overheating, energy savings, and prolonged lifespan of the hardware at hand. In addition, altering semiconductors or the excited dimer molecule allows for wavelength selection with UV LEDs and KrCl excimer lamps [16]. With respect to SARS-CoV-2 inactivation, Jureka et al. tested pulse duration times ranging from 1 to 30 min, with pulses of 2 ms after 6 s of irradiation with a broad-spectrum UV radiation source (200–700 nm); a 3-log reduction was reached with pulsed radiant exposure equalling 17.2 mJ cm^{-2} (0.033% duty rate for 5 min), while a 10-min (34.9 mJ cm^{-2} with the same duty rate) exposure resulted in a log reduction to almost undetectable levels, demonstrating that longer exposure times effectively inactivate SARS-CoV-2 [83]. Inagaki et al. [31] tested the inactivation efficacy of a 280 nm UV LED at a 50% duty rate and

compared it to 1 s and 5 s continuous UV-C on SARS-CoV-2 isolates. They obtained titer reduction up to 96.3% with 1 s continuous UV radiation and up to 99.9% reduction under 5 s of continuous UV radiation, whereas no difference was observed between pulsed and continuous irradiation [78]. Kitagawa et al. tested the inactivation efficacy of 222 nm at 0.003, 0.013, and 0.1 mW cm^{-2} with 10 s on/380 s off intervals; they observed no significant difference in the log reduction of SARS-CoV-2 at different irradiance and no significant difference between continuous and pulsed irradiation [18].

Whether UV irradiation is pulsed or continuous, radiant exposure is crucial when addressing the inactivation efficacy of microorganisms in different matrices. UV-C radiation sources emitting the highest radiant exposure in this work were the 277 nm and 280 nm UV LEDs, whereas the 260 nm UV LED emitted the lowest radiant exposure and demonstrated the lowest inactivation efficacy. For solid matrices such as food, disinfection is based on product type, surface morphology, and its water activity [15]. UV penetration depth further poses a limitation; Ngadi et al. [56] achieved a log reduction > 5 at a medium depth of 1 mm with a UV irradiance of 6.5 mW min cm^{-2}, while a log reduction of less than 1 was achieved at a medium water depth of 10 mm [84]. Reducing the microbial load of liquid matrices is further impacted by color and turbidity [15]. Recent interest in far-UV-C radiation (222 nm) is largely due to its shorter penetration depth, rendering it less harmful to mammalian tissue [44].

Data reported here support the existing dialogue that validates separate wavelengths for effective UV disinfection of identified airborne, waterborne, or foodborne pathogens. Combinations of high-performing UV-C wavelengths clearly merit further investigation if optimizing germicidal efficacies on an array of potential pathogens. Efforts to reconcile differences in testing germicidal efficacy have been made by researchers and standards development groups [69, 85–87]. The Spaulding classification system of hierarchically ranking microbial pathogens by their resistance to chemical disinfectants was first proposed over 50 years ago [88]. A re-organization of this system is long overdue and could include UVGI, TLV, and safety considerations [31, 33, 36, 87]. Recent efforts at reclassification, plotting sensitivities, and compiling germicidal efficacies for UVGI on major microbial groups, including SARS-CoV-2, have been published [11, 49, 89]. Comparatively compiled, open source UVGI data could aid readiness against the WHO's 'Disease X' in a future pandemic.

LEDs continue to attract attention for all lighting applications as they are compact in size, have flexible and narrow peak wavelengths, disposal is not as toxic as other conventional radiation sources, and have a longer life span [90]. In contrast, 222 nm emitting KrCl excimer fixtures' growing popularity is backed by safety data from healthy human volunteers and occupational workers [20, 91]. UV LED technology holds enormous potential but has yet to catch up with these findings, as few studies have reported the successful development of LEDs emitting UV-C radiation below 250 nm. Commercialization will not occur until several parameters for LEDs emitting within this range are improved, including optical output power, external quantum efficiency and wall-plug efficiency [92]. Whether from LEDs or other UV radiation sources, TLVs will dictate possible applications in health care settings and indoor public spaces. Recommended TLVs for 254 nm, 260 nm, 270 nm and 280 nm UVGI are 6 mJ cm^{-2}, 4.6 mJ cm^{-2}, 3 mJ cm^{-2}, and 3.4 mJ cm^{-2}, respectively, per day; TLV for 222 nm UV-C was recently raised to 160 mJ cm^{-2} [33, 93]. Using the UV-C radiation sources in this work, UV dosage examined far exceeds these TLVs if incorporated into lighting installations for living spaces, particularly if misused or improperly installed. Pulsed UVGI could be further investigated to reduce exposure and meet TLVs. Pulsed (248 mJ cm^{-2}) and continuous UVGI (24.8 mJ cm^{-2}) using KrCl excimers were compared to no UV-C exposure in a simulated office environment over 5-h daily exposure periods; no eye discomfort or adverse effects were reported, yet significant reductions in bacteria and fungi were observed [94].

Findings compiled in this study underline the safety risks involved in developing UV LED products destined for market without support through proper testing and accurate measurements of the manufactured radiation-emitting components. Consistent and detailed methods outlining mapping, measured wavelengths, irradiance, and radiant exposure required for meeting required log reductions might facilitate the commercialization process and support regulatory frameworks for UVGI applications that assure user safety at work and at home. Further experimental investigations and in situ studies exploring efficacies and penetration depths through different matrices are needed. All might 'shed light' on the versatile potential of designer UV LEDs that could fortify food safety or water treatment technologies, and in the current context mitigate disease spread.

5 Conclusion

Data reported herein emphasize the hierarchal sensitivities of bacteria, a human enveloped virus, and a coliform bacteriophage to UV-C radiation that have been similarly reported for chemical disinfection agents. Inactivation of the MS2 bacteriophage required the highest radiant exposure for all UV-C radiation sources and this pathogen model appears unsuitable for viral inactivation in this circumstance. A comparison of continuous and pulsed UV-C radiation demonstrates that pulsed irradiation has similar or

greater germicidal efficacy with bacterial and SARS-CoV-2 inactivation, which may be more feasible in living spaces over an extended operational or working period if TLVs are respected. Given the studied UV LEDs' lower irradiance and power outputs, in addition to the KrCl excimer's poor performance with respect to inactivating the surrogate bacteriophage MS2, further optimization is warranted with these UV-C radiation sources in other applications including water treatment, food processing, and microbial control in other settings.

Supplementary Information The online version contains supplementary material available at https://doi.org/10.1007/s43630-023-00521-2.

Acknowledgements C. Patterson, and I.S. Mahmood are gratefully acknowledged for technical support despite limiting research constraints imposed by the COVID-19 pandemic. Invaluable and long-standing support from U Technology Corporation is sincerely appreciated, as were contributions from EHC Global Inc. The authors further acknowledge the contribution of B. Charbonneau from the Infection and Inflammation core at the Centre for Phenogenomics (McGill University) for work performed in the BCL3, as well as the CL3 Technology Platform at the Research Institute of the MUHC. The authors wish to thank all members of the Biomass Production Laboratory and Kam Hammad for helpful discussions. They additionally thank P. Brunetti for help with graphics.

Funding This research was funded with collaborative support from the Natural Sciences and Engineering Research Council's Alliance Program (NSERC, ALLRP 550471-20) and U Technology Corporation. The authors acknowledge the Coronavirus Variants Rapid Response Network (CoVaRR-Net) for funding activities in the CL3 facility.

Declarations

Conflict of interest On behalf of all authors, the corresponding author states that there is no conflict of interest.

References

1. Meyerowitz, E. A., Richterman, A., Gandhi, R. T., & Sax, P. E. (2021). Transmission of SARS-CoV-2: A review of viral, host, and environmental factors. *Annals of internal medicine, 174*, 69–79. https://doi.org/10.7326/M20-5008
2. van Doremalen, N., Bushmaker, T., Morris, D. H., Holbrook, M. G., Gamble, A., Williamson, B. N., Tamin, A., Harcourt, J. L., Thornburg, N. J., & Gerber, S. I. (2020). Aerosol and surface stability of SARS-CoV-2 as compared with SARS-CoV-1. *New England Journal of Medicine, 382*, 1564–1567. https://doi.org/10.1056/nejmc2004973
3. Marquès, M., & Domingo, J. L. (2021). Contamination of inert surfaces by SARS-CoV-2: Persistence, stability and infectivity. A review. *Environmental Research, 193*, 110559. https://doi.org/10.1016/j.envres.2020.110559
4. Martins, C. P., Xavier, C. S., & Cobrado, L. (2021). Disinfection methods against SARS-CoV-2: A systematic review. *Journal of Hospital Infection*. https://doi.org/10.1016/j.jhin.2021.07.014
5. Administration, F. A. D. (2020). *Enforcement policy for sterilizers, disinfectant devices, and air purifiers during the coronavirus disease 2019 (COVID-19) public health emergency: Guidance for industry and Food and Drug Administration staff*. Retrieved from https://www.fda.gov/regulatory-information/search-fda-guidance-documents/enforcement-policy-sterilizers-disinfectant-devices-and-air-purifiers-during-coronavirus-disease.
6. Canada, G. o. (2021). *Regulating ultraviolet radiation-emitting and ozone-generating devices under the Pest Control Products Act: Overview*. Retrieved from https://www.canada.ca/en/health-canada/services/drugs-health-products/covid19-industry/disinfectanst-sanitizers-cleaners-soaps/ultra-violet-radiation-emitting-ozone-generating-devices/interim-order.html.
7. Downes, A., & Blunt, T. (1877). The influence of light upon the development of bacteria. *Nature, 16*, 218. https://doi.org/10.1038/016218a0
8. De Jager, T., Cockrell, A., & Du Plessis, S. (2017). Ultraviolet light induced generation of reactive oxygen species. *Ultraviolet Light in Human Health, Diseases, and Environment*. https://doi.org/10.1007/978-3-319-56017-5_2
9. Kim, D.-K., Kim, S.-J., & Kang, D.-H. (2017). Bactericidal effect of 266 to 279 nm wavelength UVC-LEDs for inactivation of Gram positive and Gram negative foodborne pathogenic bacteria and yeasts. *Food Research International, 97*, 280–287. https://doi.org/10.1016/j.foodres.2017.04.009
10. Luksiene, Z., & Brovko, L. (2013). Antibacterial photosensitization-based treatment for food safety. *Food Engineering Reviews, 5*, 185–199.
11. Beck, S., Rodriguez, R., Hawkins, M., Hargy, T., Larason, T., & Linden, K. (2016). Comparison of UV-induced inactivation and RNA damage in MS2 phage across the germicidal UV spectrum. *Applied Environmental Microbiology, 82*, 1468–1474. https://doi.org/10.1128/AEM.02773-15
12. Narita, K., Asano, K., Naito, K., Ohashi, H., Sasaki, M., Morimoto, Y., Igarashi, T., & Nakane, A. (2020). 222-nm UVC inactivates a wide spectrum of microbial pathogens. *Journal of Hospital Infection, 105*, 459–467. https://doi.org/10.1016/j.jhin.2020.03.030
13. Jing, Z., Lu, Z., Santoro, D., Zhao, Z., Huang, Y., Ke, Y., Wang, X., & Sun, W. (2022). Which UV wavelength is the most effective for chlorine-resistant bacteria in terms of the impact of activity, cell membrane and DNA? *Chemical Engineering Journal, 447*, 137584. https://doi.org/10.2139/ssrn.4070255
14. Ma, B., Gundy, P. M., Gerba, C. P., Sobsey, M. D., & Linden, K. G. (2021). UV inactivation of SARS-CoV-2 across the UVC spectrum: KrCl* excimer, mercury-vapor, and light-emitting-diode (LED) sources. *Applied Environmental Microbiology, 87*, e01532-01521. https://doi.org/10.1128/AEM.01532-21
15. Prasad, A., Du, L., Zubair, M., Subedi, S., Ullah, A., & Roopesh, M. (2020). Applications of light-emitting diodes (LEDs) in food processing and water treatment. *Food Engineering Reviews, 12*, 268–289. https://doi.org/10.1007/s12393-020-09221-4
16. Chen, J., Loeb, S., & Kim, J.-H. (2017). LED revolution: Fundamentals and prospects for UV disinfection applications. *Environmental Science: Water Research Technology, 3*, 188–202. https://doi.org/10.1039/C6EW00241B

17. Taylor, W., Camilleri, E., Craft, D. L., Korza, G., Granados, M. R., Peterson, J., Szczpaniak, R., Weller, S. K., Moeller, R., & Douki, T. (2020). DNA damage kills bacterial spores and cells exposed to 222-nanometer UV radiation. *Applied Environmental Microbiology, 86*, e03039-03019. https://doi.org/10.1128/aem.03039-19
18. Kitagawa, H., Nomura, T., Nazmul, T., Kawano, R., Omori, K., Shigemoto, N., Sakaguchi, T., & Ohge, H. (2021). Effect of intermittent irradiation and fluence-response of 222 nm ultraviolet light on SARS-CoV-2 contamination. *American Journal of Infection Control, 33*, 102184. https://doi.org/10.1016/j.pdpdt.2021.102184
19. Yamano, N., Kunisada, M., Kaidzu, S., Sugihara, K., Nishiaki-Sawada, A., Ohashi, H., Yoshioka, A., Igarashi, T., Ohira, A., & Tanito, M. (2020). Long-term effects of 222-nm ultraviolet radiation C sterilizing lamps on mice susceptible to ultraviolet radiation. *Photochemistry Photobiology, 96*, 853–862. https://doi.org/10.1111/php.13269
20. Fukui, T., Niikura, T., Oda, T., Kumabe, Y., Ohashi, H., Sasaki, M., Igarashi, T., Kunisada, M., Yamano, N., & Oe, K. (2020). Exploratory clinical trial on the safety and bactericidal effect of 222-nm ultraviolet C irradiation in healthy humans. *PLoS ONE, 15*, e0235948. https://doi.org/10.1371/journal.pone.0235948
21. Beck, S. E., Ryu, H., Boczek, L. A., Cashdollar, J. L., Jeanis, K. M., Rosenblum, J. S., Lawal, O. R., & Linden, K. G. (2017). Evaluating UV-C LED disinfection performance and investigating potential dual-wavelength synergy. *Water Research, 109*, 207–216. https://doi.org/10.1016/j.watres.2016.11.024
22. Song, K., Taghipour, F., & Mohseni, M. (2018). Microorganisms inactivation by continuous and pulsed irradiation of ultraviolet light-emitting diodes (UV-LEDs). *Chemical Engineering Journal, 343*, 362–370. https://doi.org/10.1016/j.cej.2018.03.020
23. Barbosa-Canovas, G. V., Pothakamury, U. R., Palou, E., & Swanson, B. G. (1997). *Nonthermal preservation of foods*. Marcel Dekker.
24. Kim, D.-K., & Kang, D.-H. (2018). Elevated inactivation efficacy of a pulsed UVC light-emitting diode system for foodborne pathogens on selective media and food surfaces. *Applied Environmental Microbiology*. https://doi.org/10.1128/aem.01340-18
25. Rowan, N. J., MacGregor, S., Anderson, J. G., Fouracre, R., McIlvaney, L., & Farish, O. (1999). Pulsed-light inactivation of food-related microorganisms. *Applied Environmental Microbiology, 65*, 1312–1315. https://doi.org/10.1128/AEM.65.3.1312-1315.1999
26. Uslu, G., Demirci, A., & Regan, J. M. (2015). Efficacy of pulsed UV-light treatment on wastewater effluent disinfection and suspended solid reduction. *Journal of Environmental Engineering, 141*, 04014090. https://doi.org/10.1061/(ASCE)EE.1943-7870.0000912
27. Vianna, P. G., Dale, C. R., Jr., Simmons, S., Stibich, M., & Licitra, C. M. (2016). Impact of pulsed xenon ultraviolet light on hospital-acquired infection rates in a community hospital. *American Journal of Infection Control, 44*, 299–303. https://doi.org/10.1016/j.ajic.2015.10.009
28. Canada, G. o. (2020b). *Ultraviolet (UV) lights and wands falsely claiming to disinfect against COVID-19*. Retrieved from https://recalls-rappels.canada.ca/en/alert-recall/ultraviolet-uv-lights-and-wands-falsely-claiming-disinfect-against-covid-19.
29. Lyons, A. B., Narla, S., Torres, A. E., Parks-Miller, A., Kohli, I., Ozog, D. M., Lim, H. W., & Hamzavi, I. H. (2021). Skin and eye protection against ultraviolet C from ultraviolet germicidal irradiation devices during the COVID-19 pandemic. *International Journal of Dermatology, 60*, 391–393. https://doi.org/10.1111/ijd.15255
30. Sengillo, J. D., Kunkler, A. L., Medert, C., Fowler, B., Shoji, M., Pirakitikulr, N., Patel, N., Yannuzzi, N. A., Verkade, A. J., & Miller, D. (2021). UV-photokeratitis associated with germicidal lamps purchased during the COVID-19 pandemic. *Ocular Immunology Inflammation, 29*, 76–80. https://doi.org/10.1080/09273948.2020.1834587
31. ACGIH. (2020, 2021). Documentation of the Threshold Limit Values® and biological exposure indices, 8th edition, with 2021 yearly update. In: *American conference of governmental industrial hygienists*. ACGIH, Cincinnati
32. ICNIRP. (2004). Guidelines on limits of exposure to ultraviolet radiation of wavelengths between 180 nm and 400 nm (incoherent optical radiation). *J Health Physics, 87*, 171–186.
33. Sliney, D. H., & Stuck, B. E. (2021). A need to revise human exposure limits for ultraviolet UV-C radiation. *Photochemistry Photobiology, 97*, 485–492. https://doi.org/10.1111/php.13402
34. WHO. (2022). *Prioritzing diseases for research and development in emergency context*. Retrieved from https://www.who.int/activities/prioritizing-diseases-for-research-and-development-in-emergency-contexts. 13 Dec 2022.
35. Ross, J., & Sulev, M. (2000). Sources of errors in measurements of PAR. *Agricultural Forest Meteorology, 100*, 103–125. https://doi.org/10.1016/S0168-1923(99)00144-6
36. Wu, B.-S., & Lefsrud, M. G. (2018). Photobiology eye safety for horticultural LED lighting: Transmittance performance of eyewear protection using high-irradiant monochromatic LEDs. *Journal of Occupational Environmental Hygiene, 15*, 133–142. https://doi.org/10.1080/15459624.2017.1395959
37. Mendoza, E. J., Manguiat, K., Wood, H., & Drebot, M. (2020). Two detailed plaque assay protocols for the quantification of infectious SARS-CoV-2. *Current Protocols in Microbiology, 57*, cpmc105. https://doi.org/10.1002/cpmc.105
38. Tavares, M. B., Souza, R. D., Luiz, W. B., Cavalcante, R., Casaroli, C., Martins, E. G., Ferreira, R. C., & Ferreira, L. (2013). Bacillus subtilis endospores at high purity and recovery yields: Optimization of growth conditions and purification method. *Current Microbiology, 66*, 279–285. https://doi.org/10.1007/s00284-012-0269-2
39. Kauffman, K. M., & Polz, M. F. J. M. (2018). Streamlining standard bacteriophage methods for higher throughput. *MethodsX, 5*, 159–172. https://doi.org/10.1016/j.mex.2018.01.007
40. Geissmann, Q. (2013). OpenCFU, a new free and open-source software to count cell colonies and other circular objects. *PLoS ONE, 8*, e54072. https://doi.org/10.1371/journal.pone.0054072
41. EPA. (2020). *EPA regulations about UV lights that claim to kill or be effective against viruses and bacteria*. Retrived from https://www.epa.gov/sites/default/files/2020-10/documents/uvlight-complianceadvisory.pdf.
42. Canada, G. o. (2020a). *Technical requirements for UV decontamination devices: Notice to manufacturers*. Retrieved from https://www.canada.ca/en/health-canada/services/drugs-health-products/covid19-industry/medical-devices/ultraviolet-decontamination-notice.html.
43. D'Souza, C., Yuk, H. G., Khoo, G. H., & Zhou, W. (2015). Application of light-emitting diodes in food production, postharvest preservation, and microbiological food safety. *Comprehensive Reviews in Food Science Food Safety, 14*, 719–740. https://doi.org/10.1111/1541-4337.12155
44. Buonanno, M., Ponnaiya, B., Welch, D., Stanislauskas, M., Randers-Pehrson, G., Smilenov, L., Lowy, F. D., Owens, D. M., & Brenner, D. J. (2017). Germicidal efficacy and mammalian skin safety of 222-nm UV light. *Radiation Research, 187*, 493–501. https://doi.org/10.1667/RR0010CC.1
45. Buonanno, M., Stanislauskas, M., Ponnaiya, B., Bigelow, A. W., Randers-Pehrson, G., Xu, Y., Shuryak, I., Smilenov, L., Owens, D. M., & Brenner, D. J. (2016). 207-nm UV light—a promising tool for safe low-cost reduction of surgical site infections. II: In-vivo safety studies. *PLoS ONE, 11*, e0138418. https://doi.org/10.1371/journal.pone.0138418

46. Kaidzu, S., Sugihara, K., Sasaki, M., Nishiaki, A., Igarashi, T., & Tanito, M. (2019). Evaluation of acute corneal damage induced by 222-nm and 254-nm ultraviolet light in Sprague-Dawley rats. *Free Radical Research, 53*, 611–617. https://doi.org/10.1080/10715762.2019.1603378
47. Kitagawa, H., Nomura, T., Nazmul, T., Omori, K., Shigemoto, N., Sakaguchi, T., & Ohge, H. (2020). Effectiveness of 222-nm ultraviolet light on disinfecting SARS-CoV-2 surface contamination. *American Journal of Infection Control, 49*, 299–301. https://doi.org/10.1016/j.ajic.2020.08.022
48. Liang, J.-J., Liao, C.-C., Chang, C.-S., Lee, C.-Y., Chen, S.-Y., Huang, S.-B., Yeh, Y.-F., Singh, K. J., Kuo, H.-C., & Lin, Y.-L. (2021). The Effectiveness of far-ultraviolet (UVC) light prototype devices with different wavelengths on disinfecting SARS-CoV-2. *Applied Sciences, 11*, 10661. https://doi.org/10.3390/app112210661
49. Hull, N. M., & Linden, K. G. (2018). Synergy of MS2 disinfection by sequential exposure to tailored UV wavelengths. *Water Research, 143*, 292–300. https://doi.org/10.1016/j.watres.2018.06.017
50. Boyce, J. M., & Donskey, C. J. (2019). Understanding ultraviolet light surface decontamination in hospital rooms: A primer. *Infection Control Hospital Epidemiology, 40*, 1030–1035. https://doi.org/10.1017/ice.2019.161
51. Fang, J., Liu, H., Shang, C., Zeng, M., Ni, M., & Liu, W. (2014). E. coli and bacteriophage MS2 disinfection by UV, ozone and the combined UV and ozone processes. *Frontiers of Environmental Science Engineering, 8*, 547–552. https://doi.org/10.1007/s11783-013-0620-2
52. Beck, S., Wright, H., Hargy, T., Larason, T., & Linden, K. (2015). Action spectra for validation of pathogen disinfection in medium-pressure ultraviolet (UV) systems. *Water Research, 70*, 27–37. https://doi.org/10.1016/j.watres.2014.11.028
53. Turgeon, N., Toulouse, M.-J., Martel, B., Moineau, S., & Duchaine, C. J. A. (2014). Comparison of five bacteriophages as models for viral aerosol studies. *Applied Environmental Microbiology, 80*, 4242–4250. https://doi.org/10.1128/aem.00767-14
54. Cadnum, J. L., Li, D. F., Jones, L. D., Redmond, S. N., Pearlmutter, B., Wilson, B. M., & Donskey, C. J. (2020). Evaluation of ultraviolet-C light for rapid decontamination of airport security bins in the era of SARS-CoV-2. *Pathogens, 5*, 133. https://doi.org/10.20411/pai.v5i1.373
55. Biasin, M., Bianco, A., Pareschi, G., Cavalleri, A., Cavatorta, C., Fenizia, C., Galli, P., Lessio, L., Lualdi, M., & Tombetti, E. (2021). UV-C irradiation is highly effective in inactivating SARS-CoV-2 replication. *Scientific Reports, 11*, 6260. https://doi.org/10.1038/s41598-021-85425-w
56. Lee, C., Park, K. H., Kim, M., & Kim, Y. B. (2022). Optimized parameters for effective SARS-CoV-2 inactivation using UVC-LED at 275 nm. *Scientific Reports, 12*, 16664. https://doi.org/10.1038/s41598-022-20813-4
57. Minamikawa, T., Koma, T., Suzuki, A., Mizuno, T., Nagamatsu, K., Arimochi, H., Tsuchiya, K., Matsuoka, K., Yasui, T., & Yasutomo, K. (2021). Quantitative evaluation of SARS-CoV-2 inactivation using a deep ultraviolet light-emitting diode. *Scientific Reports, 11*, 1–9. https://doi.org/10.1038/s41598-021-84592-0
58. Robinson, R., Mahfooz, N., Rosas-Mejia, O., Liu, Y., & Hull, N. (2022). UV222 disinfection of SARS-CoV-2 in solution. *Scientific Reports, 12*, 14545. https://doi.org/10.1038/s41598-022-18385-4
59. Alum, A., Zhao, Z., Ersan, M., Mewes, T., Barnes, M., Westerhoff, & Abbaszadegan, M. (2022). Implication of cell culture methods and biases on UV inactivation of viruses. *Journal of Virological Methods, 309*, 114610. https://doi.org/10.1016/j.jviromet.2022.114610
60. Freeman, S., Kibler, K., Lipsky, Z., Jin, S., German, G. K., & Ye, K. (2022). Systematic evaluating and modeling of SARS-CoV-2 UVC disinfection. *Scientific Reports, 12*, 1–13. https://doi.org/10.1038/s41598-022-09930-2
61. Storm, N., McKay, L. G., Downs, S. N., Johnson, R. I., Birru, D., de Samber, M., Willaert, W., Cennini, G., & Griffiths, A. (2020). Rapid and complete inactivation of SARS-CoV-2 by ultraviolet-C irradiation. *Scientific Reports, 10*, 22421. https://doi.org/10.1038/s41598-020-79600-8
62. Fedorenko, A., Grinberg, M., Orevi, T., & Kashtan, N. (2020). Survival of the enveloped bacteriophage Phi6 (a surrogate for SARS-CoV-2) in evaporated saliva microdroplets deposited on glass surfaces. *Scientific Reports, 10*, 22419. https://doi.org/10.1038/s41598-020-79625-z
63. Liao, C. H., & Shollenberger, L. (2003). Survivability and long-term preservation of bacteria in water and in phosphate-buffered saline. *Letters in Applied Microbiology, 37*, 45–50. https://doi.org/10.1046/j.1472-765x.2003.01345.x
64. Perchetti, G. A., Huang, M.-L., Peddu, V., Jerome, K. R., & Greninger, A. L. (2020). Stability of SARS-CoV-2 in phosphate-buffered saline for molecular detection. *Journal of Clinical Microbiology*. https://doi.org/10.1128/JCM.01094-20
65. Ulrich, N., Nagler, K., Laue, M., Cockell, C. S., Setlow, P., & Moeller, R. (2018). Experimental studies addressing the longevity of Bacillus subtilis spores—The first data from a 500-year experiment. *PLoS ONE, 13*, e0208425. https://doi.org/10.1371/journal.pone.0208425
66. Keshavarzfathy, M., Malayeri, A. H., Mohseni, M., & Taghipour, F. (2020). UV-LED fluence determination by numerical method for microbial inactivation studies. *Journal of Photochemistry and Photobiology A: Chemistry, 392*, 112406. https://doi.org/10.1016/j.jphotochem.2020.112406
67. Itani, N., & El Fadel, M. (2023). Microbial inactivation kinetics of UV LEDs and effect of operating conditions: A methodological critical analysis. *Science of the Total Environment*. https://doi.org/10.1016/j.scitotenv.2023.163727
68. Chen, R. Z., Craik, S. A., & Bolton, J. R. (2009). Comparison of the action spectra and relative DNA absorbance spectra of microorganisms: Information important for the determination of germicidal fluence (UV dose) in an ultraviolet disinfection of water. *Water Research, 43*, 5087–5096. https://doi.org/10.1039/C6EW00241B
69. Bolton, J. R., & Linden, K. G. (2003). Standardization of methods for fluence (UV dose) determination in bench-scale UV experiments. *Journal of Environmental Engineering, 129*, 209–215. https://doi.org/10.1061/(ASCE)0733-9372(2003)129:3(209)
70. Conzelmann, C., Gilg, A., Groß, R., Schütz, D., Preising, N., Ständker, L., Jahrsdörfer, B., Schrezenmeier, H., Sparrer, K. M., & Stamminger, T. (2020). An enzyme-based immunodetection assay to quantify SARS-CoV-2 infection. *Antiviral Research, 181*, 104882. https://doi.org/10.1016/j.antiviral.2020.104882
71. Savoie, C., & Lippé, R. (2022). Optimizing human coronavirus OC43 growth and titration. *PeerJ, 10*, e13721. https://doi.org/10.7717/peerj.13721
72. Schirtzinger, E. E., Kim, Y., & Davis, A. S. (2022). Improving human coronavirus OC43 (HCoV-OC43) research comparability in studies using HCoV-OC43 as a surrogate for SARS-CoV-2. *Journal of Virological Methods, 299*, 114317. https://doi.org/10.1016/j.jviromet.2021.114317
73. Woo, H., Beck, S. E., Boczek, L. A., Carlson, K. M., Brinkman, N. E., Linden, K. G., Lawal, O. R., Hayes, S. L., & Ryu, H. (2019). Efficacy of inactivation of human enteroviruses by dual-wavelength germicidal ultraviolet (UV-C) light emitting diodes (LEDs). *Water Research, 11*, 1131. https://doi.org/10.3390/w11061131
74. Bohrerova, Z., Shemer, H., Lantis, R., Impellitteri, C. A., & Linden, K. G. (2008). Comparative disinfection efficiency of

pulsed and continuous-wave UV irradiation technologies. *Water Research, 42*, 2975–2982. https://doi.org/10.1016/j.watres.2008.04.001
75. Elmnasser, N., Guillou, S., Leroi, F., Orange, N., Bakhrouf, A., & Federighi, M. (2007). Pulsed-light system as a novel food decontamination technology: A review. *Canadian Journal of Microbiology, 53*, 813–821. https://doi.org/10.1139/w07-042
76. Sholtes, K., & Linden, K. G. (2019). Pulsed and continuous light UV LED: Microbial inactivation, electrical, and time efficiency. *Water Research, 165*, 114965. https://doi.org/10.1016/j.watres.2019.114965
77. Fine, F., & Gervais, P. (2004). Efficiency of pulsed UV light for microbial decontamination of food powders. *Journal of Food Protection, 67*, 787–792. https://doi.org/10.4315/0362-028x-67.4.787
78. Inagaki, H., Saito, A., Kaneko, C., Sugiyama, H., Okabayashi, T., & Fujimoto, S. (2021). Rapid inactivation of SARS-CoV-2 variants by continuous and intermittent irradiation with a deep-ultraviolet light-emitting diode (DUV-LED) device. *Pathogens, 10*, 754. https://doi.org/10.3390/pathogens10060754
79. Zou, X.-Y., Lin, Y.-L., Xu, B., Cao, T.-C., Tang, Y.-L., Pan, Y., Gao, Z.-C., & Gao, N.-Y. (2019). Enhanced inactivation of *E. coli* by pulsed UV-LED irradiation during water disinfection. *Science of the Total Environment, 650*, 210–215. https://doi.org/10.1016/j.scitotenv.2018.08.367
80. Sommer, R., Haider, T., Cabaj, A., Pribil, W., & Lhotsky, M. (1998). Time dose reciprocity in UV disinfection of water. *Water Science Technology, 38*, 145–150. https://doi.org/10.1016/S0273-1223(98)00816-6
81. Song, K., Mohseni, M., & Taghipour, F. (2019). Mechanisms investigation on bacterial inactivation through combinations of UV wavelengths. *Water Research, 163*, 114875. https://doi.org/10.1016/j.watres.2019.114875
82. Nyangaresi, P. O., Rathnayake, T., & Beck, S. E. (2023). Evaluation of disinfection efficacy of single UV-C, and UV-A followed by UV-C LED irradiation on *Escherichia coli*, *B. spizizenii* and MS2 bacteriophage, in water. *Science of the Total Environment, 859*, 160256. https://doi.org/10.1016/j.scitotenv.2022.160256
83. Jureka, A. S., Williams, C. G., & Basler, C. F. (2021). Pulsed broad-spectrum UV light effectively inactivates SARS-CoV-2 on multiple surfaces and N95 material. *Viruses, 13*, 460. https://doi.org/10.3390/v13030460
84. Ngadi, M., Smith, J. P., & Cayouette, B. (2003). Kinetics of ultraviolet light inactivation of *Escherichia coli* O157:H7 in liquid foods. *Journal of the Science of Food Agriculture, 83*, 1551–1555. https://doi.org/10.1002/jsfa.1577
85. Bolton, J., Mayor-Smith, I., & Linden, K. (2015). Rethinking the concepts of fluence (UV dose) and fluence rate: The importance of photon-based units–a systemic review. *Photochemistry Photobiology, 91*, 1252–1262. https://doi.org/10.1111/php.12512
86. ASTM. (2018). *E3135-18. Standard practice for determining antimicrobial efficacy of ultraviolet germicidal irradiation against microorganisms on carriers with simulated soil*.
87. McDonnell, G., & Burke, P. (2011). Disinfection: Is it time to reconsider Spaulding? *Journal of Hospital Infection, 78*, 163–170. https://doi.org/10.1016/j.jhin.2011.05.002
88. Spaulding, E. H. (1968). *Chemical disinfection of medical and surgical materials*. Lea & Febiger.
89. Schuit, M. A., Larason, T. C., Krause, M. L., Green, B. M., Holland, B. P., Wood, S. P., Grantham, S., Zong, Y., Zarobila, C. J., & Freeburger, D. L. (2022). SARS-CoV-2 inactivation by ultraviolet radiation and visible light is dependent on wavelength and sample matrix. *Journal of Photochemistry Photobiology B: Biology, 233*, 112503. https://doi.org/10.1016/j.jphotobiol.2022.112503
90. Rattanakul, S., & Oguma, K. (2018). Inactivation kinetics and efficiencies of UV-LEDs against *Pseudomonas aeruginosa*, *Legionella pneumophila*, and surrogate microorganisms. *Water Research, 130*, 31–37. https://doi.org/10.1016/j.watres.2017.11.047
91. Sugihara, K., Kaidzu, S., Sasaki, M., Ichioka, S., Takayanagi, Y., Shimizu, H., Sano, I., Hara, K., & Tanito, M. (2022). One-year ocular safety observation of workers and estimations of microorganism inactivation efficacy in the room irradiated with 222-nm far ultraviolet-C lamps. *Photochemistry Photobiology*. https://doi.org/10.1111/php.13710
92. Kneissl, M., Seong, T.-Y., Han, J., & Amano, H. (2019). The emergence and prospects of deep-ultraviolet light-emitting diode technologies. *Nature Photonics, 13*, 233–244. https://doi.org/10.1038/s41566-019-0359-9
93. ACGIH. (2021). *2021 Threshold limit values and biological exposure indices*. ACGIH.
94. Kousha, O., O'Mahoney, P., Hammond, R., Wood, K., & Eadie, E. (2023). 222 nm Far-UVC from filtered krypton-chloride excimer lamps does not cause eye irritation when deployed in a simulated office environment. *Photochemistry and Photobiology*. https://doi.org/10.1111/php.13805